AD_____

Award Number: DAMD17-00-1-0517

TITLE: A Quantitative MRI Study of Prostate Cancer Before and After Radiation Therapy

PRINCIPAL INVESTIGATOR: David L.Buckley, Ph.D.

CONTRACTING ORGANIZATION: The University of Manchester
Manchester, M13 9PL United Kingdom

REPORT DATE: May 2002

TYPE OF REPORT: Annual

PREPARED FOR: U.S. Army Medical Research and Materiel Command
Fort Detrick, Maryland 21702-5012

DISTRIBUTION STATEMENT: Approved for Public Release;
Distribution Unlimited

The views, opinions and/or findings contained in this report are those of the author(s) and should not be construed as an official Department of the Army position, policy or decision unless so designated by other documentation.

20021024 013

REPORT DOCUMENTATION PAGE

Form Approved
OMB No. 074-0188

Public reporting burden for this collection of information is estimated to average 1 hour per response, including the time for reviewing instructions, searching existing data sources, gathering and maintaining the data needed, and completing and reviewing this collection of information. Send comments regarding this burden estimate or any other aspect of this collection of information, including suggestions for reducing this burden to Washington Headquarters Services, Directorate for Information Operations and Reports, 1215 Jefferson Davis Highway, Suite 1204, Arlington, VA 22202-4302, and to the Office of Management and Budget, Paperwork Reduction Project (0704-0188), Washington, DC 20503

1. AGENCY USE ONLY (Leave blank)	2. REPORT DATE	3. REPORT TYPE AND DATES COVERED
	May 2002	Annual (15 Apr 01 - 14 Apr 02)

4. TITLE AND SUBTITLE

A Quantitative MRI Study of Prostate Cancer Before and After Radiation Therapy

5. FUNDING NUMBERS

DAMD17-00-1-0517

6. AUTHOR(S)

David L.Buckley, Ph.D.

7. PERFORMING ORGANIZATION NAME(S) AND ADDRESS(ES)

The University of Manchester
Manchester, M13 9PL United Kingdom

E-Mail: david.buckley@man.ac.uk

8. PERFORMING ORGANIZATION REPORT NUMBER

9. SPONSORING / MONITORING AGENCY NAME(S) AND ADDRESS(ES)

U.S. Army Medical Research and Materiel Command
Fort Detrick, Maryland 21702-5012

10. SPONSORING / MONITORING AGENCY REPORT NUMBER

11. SUPPLEMENTARY NOTES

Report contains color

12a. DISTRIBUTION / AVAILABILITY STATEMENT

Approved for Public Release; Distribution Unlimited

12b. DISTRIBUTION CODE

13. Abstract ***(Maximum 200 Words)*** *(abstract should contain no proprietary or confidential information)*

The purpose of the study is to examine the influence of external beam radiation on the prostate and prostate cancer using novel quantitative MRI techniques. Twenty-one men, previously diagnosed with prostate cancer, will be studied using T2 relaxation mapping and contrast agent kinetic methods before and after treatment by radiotherapy. The MRI findings will be correlated with biochemical (prostate specific antigen) progression and biopsy results. At the end of year 2 all steps are in place for the assessment and analysis of the clinical data. Ten patients have thus far been studied and a preliminary analysis of their data has been undertaken. The data is both complete and of a high quality. The findings described in year 1 have been published and there is considerable interest from the MR community in the results generated.

14. Subject Terms (keywords previously assigned to proposal abstract or terms which apply to this award)

Magnetic resonance imaging; contrast agents; radiation therapy; angiogenesis; biological modeling

15. NUMBER OF PAGES
16

16. PRICE CODE

17. SECURITY CLASSIFICATION OF REPORT	18. SECURITY CLASSIFICATION OF THIS PAGE	19. SECURITY CLASSIFICATION OF ABSTRACT	20. LIMITATION OF ABSTRACT
Unclassified	Unclassified	Unclassified	Unlimited

Table of Contents

INTRODUCTION

The following report details the results of year two of a quantitative magnetic resonance imaging (MRI) study of prostate cancer before and after radiation therapy. The study aims to examine the influence of external beam radiation on the prostate and prostate cancer using novel quantitative MRI techniques. Twenty-one men, previously diagnosed with prostate cancer, will be studied using T2 relaxation mapping and contrast agent kinetic methods before and after treatment by radiotherapy. The MRI findings will be correlated with biochemical (prostate specific antigen) and biopsy results.

BODY

The following section summarises the research accomplishments associated with the tasks outlined in the approved Statement of Work. Despite the delays experienced in transferring the grant funding from the University of Florida to the University of Manchester and the subsequent delay in obtaining Human Subjects approval (detailed in the Year 1 annual report), significant progress has been made with the Statement of Work. The research accomplishments associated with each of the tasks outlined are described below.

Task 1.

Months 1-6. To complete the imaging sequence design and testing. (specific aims 1 and 2).

a. The T1/T2 phantom will be constructed.
b. Calibration of the dynamic imaging sequences (proton density weighted + T1-weighted sequences)
c. Optimization of the FSE, T2 imaging sequence.
d. Selection of dynamic and T2 imaging sequences. Finalize imaging protocol.

As noted in the Year 1 report, with the cooperation of Drs. Steve Blackband, Amanda Barry (Post-Doctoral Research Assistant) and Geoff Parker (Research Fellow working on related studies), all elements of *Task 1* were successfully completed.

Task 2.

Months 7-12. Dynamic data simulation and model development (specific aim 1). Software development (specific aims 1 and 2).

a. Compare simulated data with patient data (both existing and data being acquired in task 3).
b. Error propagation analysis of models under test.
c. Software development. T2 maps and dynamic data analysis.

a. &
b. Significant progress continues to be made following the very positive start outlined in the Year 1 report. In summary, the model of St. Lawrence and Lee [1] has been implemented for the assessment of tissue perfusion, blood volume and Gd-DTPA extraction. However, it may not be appropriate for pixel-by-pixel analysis (due to its complex nature [2]). The model of Tofts and Kermode [3] has been selected for generating tissue uptake maps [4]. Details of these ongoing studies are included in the Appendices:

    i. Appendix 1. The manuscript entitled, "Uncertainty in the analysis of tracer kinetics using dynamic contrast-enhanced T1-weighted MRI", dealing with the accuracy of three potential models for data analysis, was published in *Magnetic Resonance in Medicine* in early 2002 [2]. The manuscript compares known simulated data with example experimental data and concludes that the St. Lawrence model is the most accurate of those tested.

ii. Appendix 2. An abstract entitled, "The influence of transcapillary water exchange on the analysis of tracer kinetics in dynamic Gd-DTPA-enhanced T1-weighted MRI" was accepted for presentation at the 10th Annual Meeting of the International Society for Magnetic Resonance in Medicine (Honolulu, May 2002). The letter deals with important issues related to the assessment of tissue concentration of Gd-DTPA and follows from both the work described in Appendix 1 and the recently published *Letter to the Editor* described in the Year 1 Annual Report [5]. Importantly, the findings help to highlight those kinetic parameters that can and cannot be accurately determined *in vivo*.

c. The areas of work including software development and data analysis have benefited immensely from the recent appointments (within the Division of Imaging Science & Biomedical Engineering) of Dr. Geoff Parker (Research Fellow) and Mr. Caleb Roberts (Post-graduate Research Assistant). As noted in last years Report, Dr. Parker has spent a number of years developing techniques and software for dynamic data analysis[4]. With the loss of Dr. Barry in late 2001 (Dr. Barry left Manchester following her marriage), it was decided to employ her unused salary to pay a fraction of Dr. Parker and Mr. Roberts salaries. In this way their expertise and on-going experience (in related oncological studies) could be applied directly to this work. Dr. Parker has written software to model and display, as colour coded physiological parameter maps [4, 6], the dynamic data. Mr. Roberts has processed all the data so far collected in the study and generated the parameter maps (see below). These maps have been used to guide Drs. Hutchinson and Buckley in their region of interest analysis.

Task 3.

Months 7-18. Patient recruitment (21 patients) and examination for pretreatment phase of specific aim 3.

a. In collaboration with Pathology, examine recent biopsy data for potential patients.
b. Select patients (in collaboration with Mr. Clarke) for the study. Obtain written, informed consent.
c. Acquire data from the 1.5 T system. Backup (optical disks) and transfer data to laboratory.
d. Stain and reanalyze biopsy specimens.

a. &
b. Patient recruitment got underway in the summer of 2001. Initial attempts to select patients were hampered by staff shortages, a competing radiotherapy trial and reorganisation in the Oncology clinic (following recruitment of the first two patients there was a significant lull). However, by March 2002 10 patients had been recruited to the study and had provided informed consent. It is anticipated that the remaining 11 patients will be accrued before September 2002. This seems very realistic given recent accrual rates: 2 patients in January; 2 patients in February; 4 patients in March.
c. Data were acquired from the first two patients in the summer of 2001. The lull in patient recruitment was followed by an upgrade to the MR system which necessitated testing to confirm the prostate protocol could be maintained. Patients 3 to 10 were subsequently imaged at the beginning of 2002. All data were backed-up on both optical disk and CD. The finalised imaging protocol is outlined below:
    1. Scout images
    2. Coronal and transverse T1-weighted SE images of the pelvis.
    3. Sagittal and transverse T2-weighted images of the prostate.
    4. Transverse T2 images for quantitative T2-mapping.
    5. 3D volume acquisitions (at 2, 10, 20 and 30 degree flip angles) for T1 quantitation.
    6. 3D dynamic volume acquisition with 0.1 mmol/kg Gd-DTPA-BMA injection.
    7. Post-contrast transverse T1-weighted SE images of the pelvis.

    Other than a few minor changes to the dynamic sequence timing, all patients underwent the same protocol and data of a high quality were acquired from all 10. Examples of some of the images acquired are shown below.
d. Dr. West and Mr. Clarke decided that the most efficient and appropriate means of analysing the biopsy specimens was to process them as a batch. As such, the specimens have not yet been analysed but will be assessed following recruitment of all 21 patients.

Task 4.

Months 13-24. Data analysis, pretreatment phase.

a. Generation of Gd-DTPA concentration maps, uptake rate/max uptake maps and T2 maps.
b. Image review with biopsy results. Preliminary identification of cancer/BPH/normal tissue.
c. Region of interest analysis. Model fitting (dynamic data).

a, b, c In collaboration with Dr. Parker and Mr. Roberts, maps of the following parameters were generated for each study: Baseline T1 and T2, contrast agent volume transfer constant, rate constant and interstitial volume fraction [7]. Examples are shown below (Figs. 1, 2 and 3).

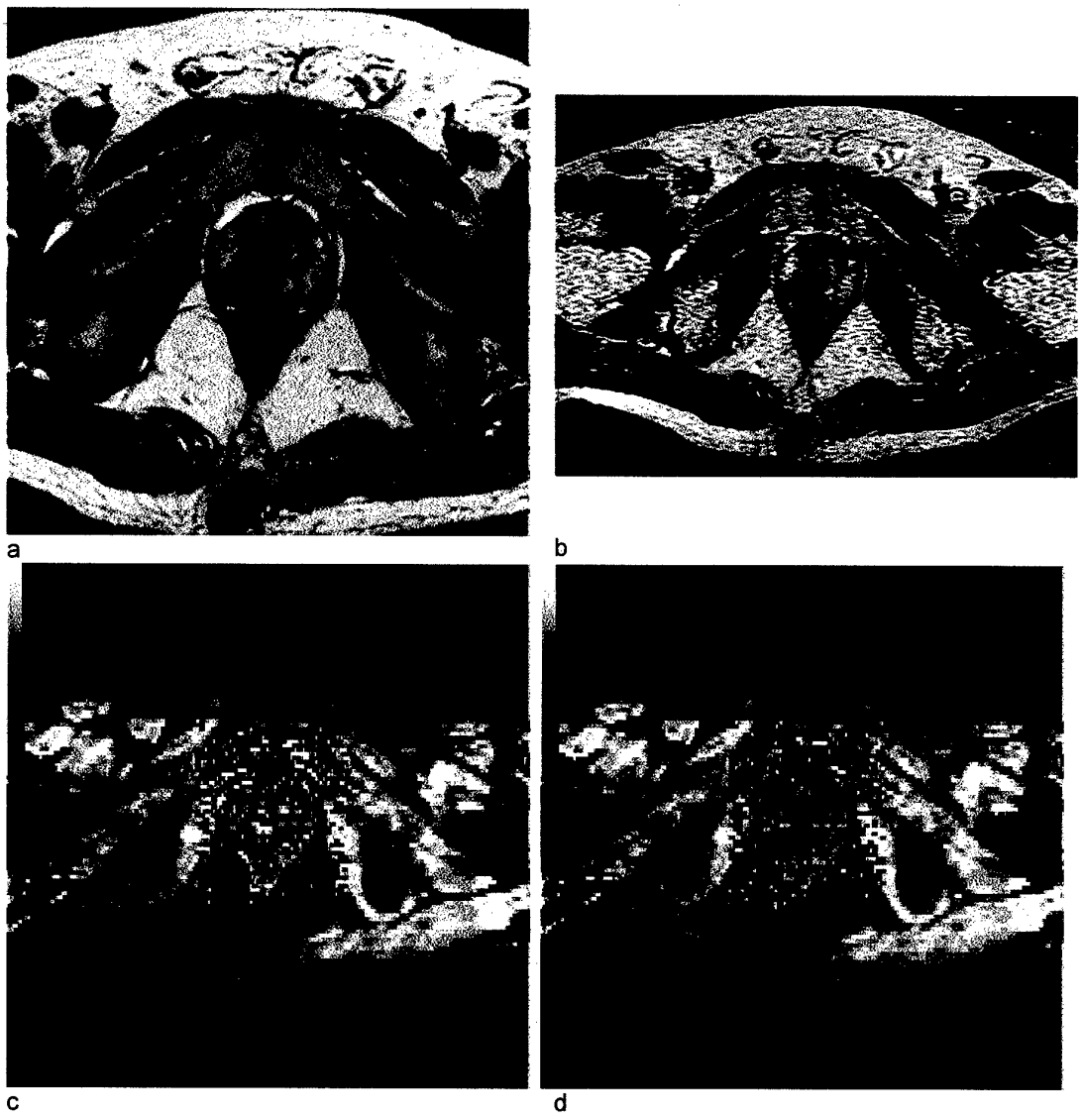

Figure 1. (a) T2-weighted image of a patient with prostate cancer (posterior right aspect of the gland). (b) T2 map (scaled between 0 and 200 ms) of a similar transverse section. The suspect region is clearly identified as having a low T2. (c) Colour map of K^{trans} parameter (limited to the area of the prostate gland) overlaid onto a T1 map (greyscale). The suspect region has higher Gd-DTPA transfer rates than the contralateral peripheral zone. (d) Colour map of v_e parameter (limited to the area of the prostate gland) overlaid onto a T1 map (greyscale).

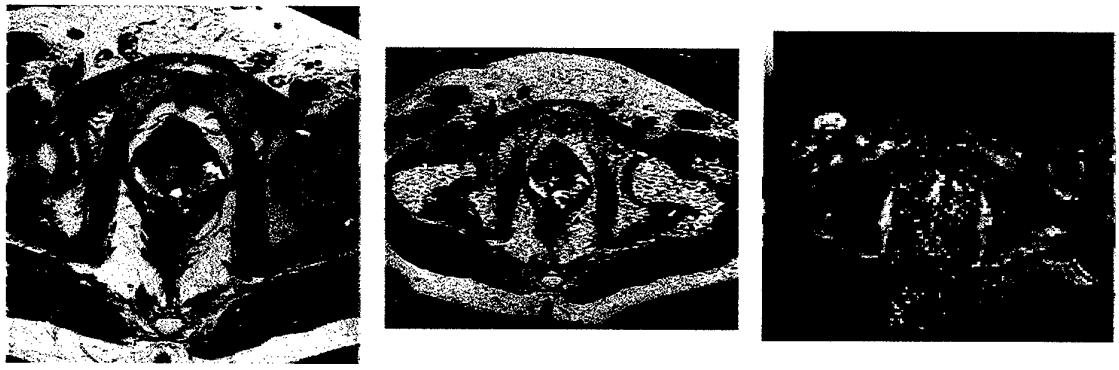

a b c

Figure 2. (a) T2-weighted image of a patient with prostate cancer (left aspect of the gland). (b) T2 map (scaled between 0 and 200 ms) of a similar transverse section. The suspect region is identified as having a low T2 while post-biopsy cystic changes have long T2. (c) Colour map of K^{trans} parameter (limited to the area of the prostate gland) overlaid onto a T1 map (greyscale). The suspect region (around the cystic changes) has high Gd-DTPA transfer rates.

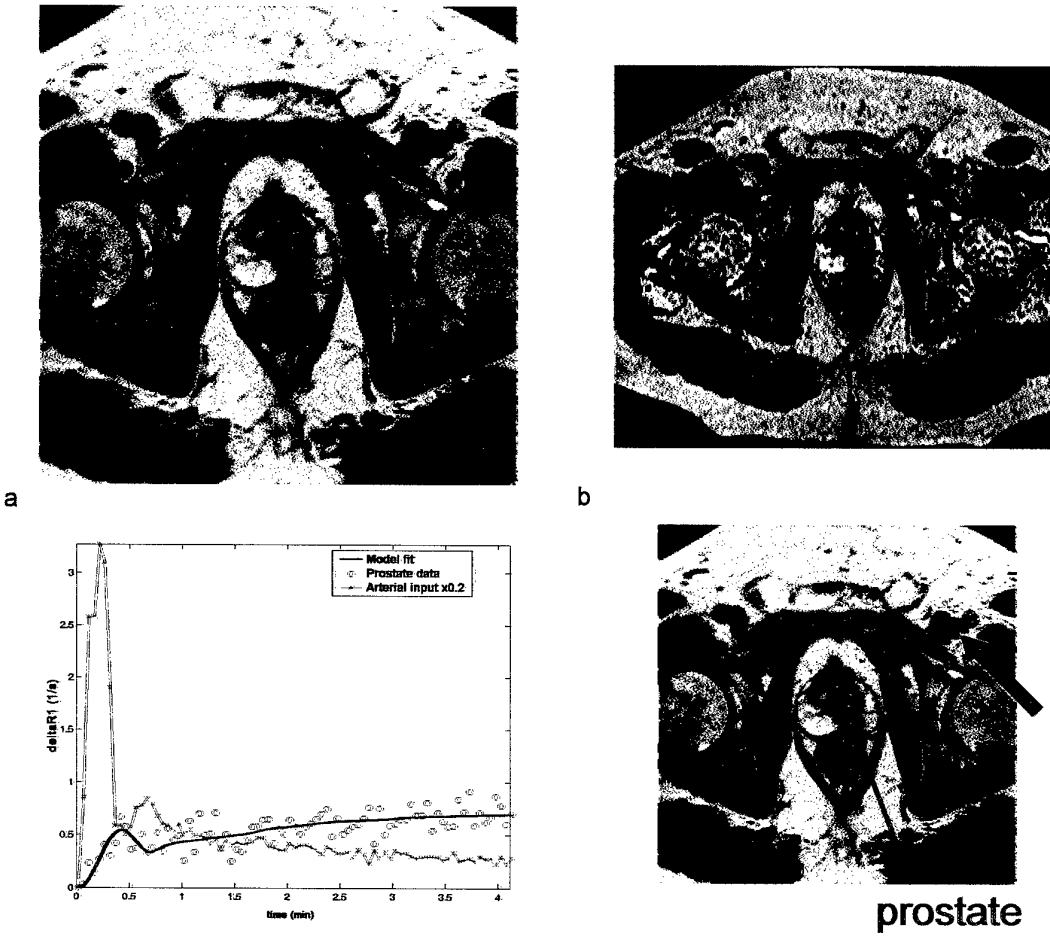

a b c

Figure 3. (a) T2-weighted image of a patient with prostate cancer (posterior left). (b) T2 map of a similar section. (c) 1/T1 changes with time in regions of interest within the femoral artery (blue circles) and prostate gland (red circles). A model fit to the prostate data (red line) using the femoral artery data as tissue input resulted in estimates of blood flow (0.14 ml/min/g), blood volume (0.05 ml/g), interstitial volume (0.28 ml/g) and capillary permeability-surface area product (0.18 ml/min/g).

Task 5.

Months 19-30. Patient follow-up (21 patients) and examination for post-treatment phase of specific aim 3.

a. Request 2nd examination for each of the patients studied in task 3.
b. Acquire data from the 1.5 T system. Backup (optical disks) and transfer data to laboratory.

Task 6.

Months 19-30. Data analysis, post-treatment phase.

a. Generation of Gd-DTPA concentration maps, uptake rate/max uptake maps and T2 maps.
b. Image review with previous MRI and biopsy results. Identification of cancer/BPH/normal tissue.
c. Region of interest analysis. Model fitting (dynamic data).

The delays experienced at the outset of the project have delayed progress with *Tasks 5 and 6.* Since the first patient was not examined until July 2001 it is not anticipated that work on these tasks will begin until Summer 2002. However, close collaboration between Dr. John Logue (Clinical Oncologist) and Mr. Noel Clarke (Urologist) facilitated by Dr. Logue's Research Nurse have helped to put in place procedures for tracking patients through their treatment, MR follow-up and subsequent biopsy.

KEY RESEARCH ACCOMPLISHMENTS

- Implementation of software tools for T1 and T2 measurement, dynamic data analysis and parameter map creation.
- Assessment of the errors associated with data collection (water exchange) and data analysis (model comparisons).
- Successful protocol implementation and acquisition of complete data from 10 patients.
- Identification and analysis of regional uptake kinetics by the model of St. Lawrence & Lee [1].

REPORTABLE OUTCOMES:

The outcomes are listed in chronological order:

1. September 2001.
Invited lecture, "D.L. Buckley, Modelling tracer kinetics in MRI". Keynote Presentation at the European Congress of Medical Physics and Clinical Engineering, Belfast.

2. February 2002.
Abstract, "D.L. Buckley, The influence of transcapillary water exchange on the analysis of tracer kinetics in dynamic Gd-DTPA-enhanced T1-weighted MRI", accepted for presentation at the International Society for Magnetic Resonance in Medicine (ISMRM) 10th Annual Meeting.

3. March 2002.
Paper, "D.L. Buckley, Uncertainty in the analysis of tracer kinetics using dynamic contrast-enhanced T1-weighted MRI", published in the journal *Magnetic Resonance in Medicine*, volume 47, pages 601-606, 2002.

4. April 2002.
Invited lecture, "D.L. Buckley, Modelling tracer kinetics using MRI". Presented to scientists at Sunnybrook and Women's Health Sciences Centre, University of Toronto, Toronto, Canada.

CONCLUSIONS

A successful year building on the groundwork of year 1. Patient data has been successfully obtained in all 10 studies to date and software, analysis tools and personnel are all in place for assessment of these data. Preliminary analysis of these data suggest that data quality is good and all the parameters that might have been examined will indeed be available for assessment.

The findings to date are extremely promising. For the first time (to our knowledge), we are using MRI to estimate blood flow, blood volume and capillary permeability of the prostate *in vivo*. The only similar work elsewhere in the world has been undertaken using PET [8] and CT [9]. The techniques under development are being used in parallel studies in the brain (where cross-fertilisation of ideas has helped to develop the water exchange studies). The work is also generating interest amongst the leading international groups. The studies' findings have been presented (as a Keynote Address) at a recent European meeting and by invitation at the University of Toronto. Furthermore, Prof. Paul Tofts (a lead investigator in the field of contrast agent kinetics, see refs. below) has shown considerable interest in the project. Thus, despite the delayed introduction of the project, progress has been significant.

REFERENCES

1. St Lawrence KS, Lee TY. An adiabatic approximation to the tissue homogeneity model for water exchange in the brain: I. Theoretical derivation. J Cereb Blood Flow Metab 1998;18:1365-1377.
2. Buckley DL. Uncertainty in the analysis of tracer kinetics using dynamic contrast-enhanced T1-weighted MRI. Magn Reson Med 2002;47:601-606.
3. Tofts PS, Kermode AG. Measurement of the blood-brain barrier permeability and leakage space using dynamic MR imaging. 1. Fundamental concepts. Magn Reson Med 1991;17:357-367.
4. Parker GJM, Suckling J, Tanner SF, Padhani AR, Revell PB, Husband JE, Leach MO. Probing tumor microvascularity by measurement, analysis and display of contrast agent uptake kinetics. J Magn Reson Imaging 1997;7:564-574.
5. Buckley DL. Transcytolemmal water exchange and its affect on the determination of contrast agent concentration in vivo. Magn Reson Med 2002;47:420-421.
6. Buckley DL, Kerslake RW, Blackband SJ, Horsman A. Quantitative analysis of multislice Gd-DTPA enhanced dynamic MR images using an automated simplex minimization procedure. Magn Reson Med 1994;32:646-651.
7. Tofts PS, Brix G, Buckley DL, Evelhoch JL, Henderson E, Knopp MV, Larsson HB, Lee TY, Mayr NA, Parker GJ, Port RE, Taylor J, Weisskoff RM. Estimating kinetic parameters from dynamic contrast-enhanced T1-weighted MRI of a diffusable tracer: Standardized quantities and symbols. J Magn Reson Imaging 1999;10:223-232.
8. Inaba T. Quantitative measurements of prostatic blood flow and blood volume by positron emission tomography. J Urol 1992;148:1457-1460.
9. Koh TS, Zeman V, Darko J, Lee TY, Milosevic MF, Haider M, Warde P, Yeung IWT. The inclusion of capillary distribution in the adiabatic tissue homogeneity model of blood flow. Phys Med Biol 2001;46:1519-1538.

NOTES

Magnetic Resonance in Medicine 47:601–606 (2002)
DOI 10.1002/mrm.10080

Uncertainty in the Analysis of Tracer Kinetics Using Dynamic Contrast-Enhanced T_1-Weighted MRI

David L. Buckley*

In recent years a number of physiological models have gained prominence in the analysis of dynamic contrast-enhanced T_1-weighted MRI data. However, there remains little evidence to support their use in estimating the absolute values of tissue physiological parameters such as perfusion, capillary permeability, and blood volume. In an attempt to address this issue, data were simulated using a distributed pathway model of tracer kinetics, and three published models were fitted to the resultant concentration-time curves. Parameter estimates obtained from these fits were compared with the parameters used for the simulations. The results indicate that the use of commonly accepted models leads to systematic overestimation of the transfer constant, K^{trans}, and potentially large underestimates of the blood plasma volume fraction, V_p. In summary, proposals for a practical approach to physiological modeling using MRI data are outlined. Magn Reson Med 47:601–606, 2002.
© 2002 Wiley-Liss, Inc.

Key words: perfusion; gadolinium; carcinoma; kinetic modeling; capillary permeability; blood volume

The last decade has seen a rapid development in the use of dynamic contrast-enhanced T_1-weighted MRI in medicine. In tandem with the technological advances that have enabled improved data acquisition, a number of investigators have employed physiological models to facilitate data interpretation. While the use of these models has found numerous applications (e.g., in studies of tumor physiology (1) and myocardial perfusion (2)), and a number of groups have assessed the potential of model parameters as surrogate markers (3,4), little has been published that addresses the direct interpretation of these results. Specifically, how do the estimates obtained using the various models compare with the physiological parameters they purport to measure?

This is not a simple question to address since it is often difficult to identify a reliable "gold standard." Many investigators compare their results with those obtained with positron emission tomography (PET). However, PET shares many of the basic models employed in MRI (5). Similarly, data simulation exercises using Monte-Carlo techniques designed to assess accuracy and precision in parameter estimation often utilize the same model to both generate and analyze the data (6,7). In this way, the sensitivity of the estimates to experimental variables, such as noise and sampling frequency, is assessed but little is revealed about the physiological significance of the resultant parameter estimates.

A physiological model incorporating multiple parallel pathways and heterogeneous flow was used to simulate data of a realistic nature to which simplified models were fitted. The experiment was designed to assess the accuracy of the models themselves, not the quality of the data to which they are fitted (in terms of noise, sampling frequency, etc.), since data quality is essentially an experimental variable. Furthermore, this study was restricted to those models dealing with a contrast agent that diffuses out of the vascular space (thereby incorporating capillary permeability as a model parameter). Many of the issues associated with the analysis of data from susceptibility contrast studies, which typically assume that the contrast agent remains intravascular, have been investigated in previous studies (e.g., Refs. 7 and 8). Data were simulated using the distributed pathway model of tracer kinetics called the multiple indicator, multiple path, indicator dilution 4 region model (MMID4), made available by the National Simulation Resource (Department of Bioengineering, University of Washington). These data were subsequently analyzed using three different tracer kinetic models, and the parameter estimates obtained were compared with the physiological variables used in the MMID4 model.

Out of necessity, only a few models and the underlying assumptions that support these models can be examined. The use of a fixed input function (originally proposed by Tofts and Kermode (9)) is known to introduce considerable error into the estimate of the capillary permeability-surface area product (10). Given this, the following analyses assume that the arterial input function has been measured. Although techniques to achieve this are not yet in common use, an increasing number of investigators are developing practical methods for doing so (11,12).

METHODS

Data Simulation

Tissue residue curves were simulated using the MMID4. This model (described in detail in Refs. 13 and 14) accounts for flow dispersion and heterogeneity, and includes capillaries modeled as axially distributed blood–tissue exchange units. A plasma concentration-time curve was simulated as an input to the model. The amplitude and shape of the curve were based upon measurements made in the

Imaging Science and Biomedical Engineering, University of Manchester, Manchester, UK.

Grant sponsor: U.S. Department of Defense Prostate Cancer Research Program; Grant number: PC991154; Grant sponsor: NIH; Grant number: RO1 NS36992.

*Correspondence to: David L. Buckley, Ph.D., Imaging Science and Biomedical Engineering, University of Manchester, Stopford Building, Oxford Road, Manchester M13 9PT, UK. E-mail: david.buckley@man.ac.uk

Received 6 September 2001; revised 22 October 2001; accepted 22 October 2001.

© 2002 Wiley-Liss, Inc.

descending aorta of volunteers following bolus injection of Gd-DTPA (11). Reference data for comparison with the simulated residue curves were obtained from MR studies of human brain, breast, and prostate tumors (15).

Numerous parameters determine the behavior of the MMID4 model. Delay and dispersion of the arterial input were set to zero. Contrast agent in nonexchanging vessels (arteries, arterioles, venules, and veins) may contribute to the tissue residue function. However, such vessels were excluded in this study, as the tumors of interest are likely to contain a predominance of newly formed, leaky vessels (16). Flow heterogeneity was modeled by apportioning flow through 20 parallel pathways according to a right-skewed lagged normal density distribution (14). For the sake of clarity a tissue density of 1 g/ml was assumed for all model analyses (17). Other than mean plasma flow (F_p) the only parameters that were adjusted in the simulations were those associated with blood–tissue exchange: capillary plasma volume (V_p), capillary permeability-surface area product (PS), and interstitial volume (V_e).

Model Fitting

Three models were chosen for assessment. Model 1, the modified Kety model (18), was essentially applied to MRI data by both Larsson et al. (19) and Tofts and Kermode (9):

$$C_{tis}(t) = EF_p \int_0^t C_p(u)\exp\left(\frac{-EF_p}{V_e}(t-u)\right)du \qquad [1]$$

where C_{tis} and C_p are the concentrations of contrast agent in the tissue of interest and plasma, respectively, and the extraction fraction, $E = 1 - \exp(-PS/F_p)$. In accord with recent standardization, it is important to stress that the product EF_p may also be referred to as K^{trans} (20). Model 2 resembles the first, but includes a vascular term (17) and has been used to analyze MR data in a number of studies (2,6):

$$C_{tis}(t) = V_pC_p(t) + EF_p \int_0^t C_p(u)\exp\left(\frac{-EF_p}{V_e}(t-u)\right)du. \qquad [2]$$

Model 3, recently described by St. Lawrence and Lee (21), potentially enables the estimation of F_p and PS separately:

$$C_{tis}(t) = F_p \int_0^\tau C_p(t-u)du + EF_p \int_\tau^t C_p(u) \times \exp\left(\frac{-EF_p}{V_e}(t-u-\tau)\right)du \qquad [3]$$

where τ is the mean capillary transit time ($= V_p/F_p$). Model 1 has two unknown parameters that may be estimated by curve fitting: the product EF_p and the interstitial volume V_e. Model 2 has three unknown parameters: the product EF_p, the interstitial volume V_e, and the plasma volume V_p. Model 3 contains four unknown parameters that may be estimated by curve fitting: F_p, E, V_e, and τ. From these, the parameters PS and V_p may be evaluated.

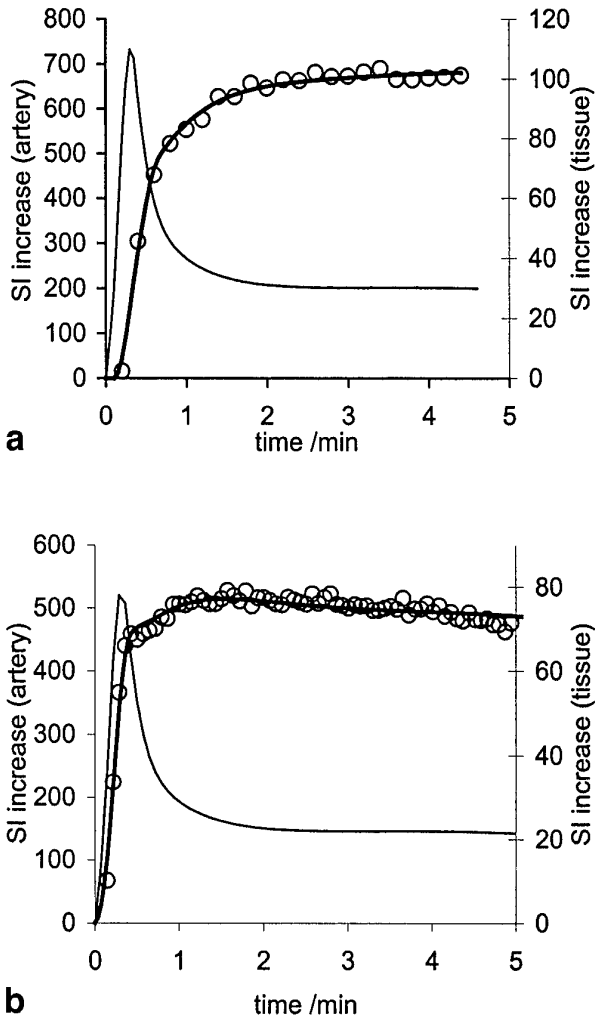

FIG. 1. Representative signal-time curves used for simulations. Tissue signal-time curves (bold lines) simulated using an assumed arterial input function (faint lines), MMID4, and the physiological parameters: (**a**) F_p, 0.57 ml/g/min; V_p, 0.06 ml/g; PS, 0.33 ml/g/min; V_e, 0.45 ml/g; and (**b**) F_p, 1.2 ml/g/min; V_p, 0.08 ml/g; PS, 0.34 ml/g/min; V_e, 0.40 ml/g. Reference data (open circles) were obtained from studies of (**a**) a breast tumor and (**b**) a meningioma.

Simulated data were generated in two series. The first series was designed to be representative of data acquired from a breast tumor, and the second was representative of data acquired from a meningioma (Fig. 1). Baseline values selected for V_p and V_e were based on estimates from the literature. These values were then held fixed while MMID4, with only F_p and PS as free parameters, was fitted to the reference data. Best-fit estimates of F_p and PS combined with the choices of V_p and V_e were then used as baseline values for the simulated data. In each case points were calculated with a sampling frequency of one acquisition per second over a total sampling period of 5 min. Twenty-six tissue residue curves were produced using the range of parameter values outlined in Table 1 (Fig. 2). In each case one parameter value (F_p, V_p, or PS) was modified from the baseline values per curve. Four values of each

Table 1
Values of the Adjustable Kinetic Parameters Describing the Behavior of MMID4 Used to Simulate 26 Different Tissue Residue Curves

	Baseline	Exps. 2–5	Exps. 6–9	Exps. 10–13
(a) Data representative of a breast tumor				
F_p (ml/min/g)	0.57	0.17, 0.37, 0.77, 0.97	0.57	0.57
V_p (ml/g)	0.06	0.06	0.0001, 0.03, 0.09, 0.12	0.06
PS (ml/min/g)	0.33	0.33	0.33	0.01, 0.17, 0.49, 0.65
V_e (ml/g)	0.45	0.45	0.45	0.45
(b) Data representative of a meningioma				
F_p (ml/min/g)	1.2	0.4, 0.8, 1.6, 2.0	1.2	1.2
V_p (ml/g)	0.08	0.08	0.0001, 0.04, 0.12, 0.16	0.08
PS (ml/min/g)	0.34	0.34	0.34	0.0, 0.17, 0.51, 0.68
V_e (ml/g)	0.4	0.4	0.4	0.4

The remaining parameters associated with MMID4 were held fixed (see text). A representative selection of the resultant tissue residue curves is shown in Fig. 2.

parameter were chosen in addition to the baseline values; thus, 13 curves were generated per series. Each of the three models in turn was fitted to the 26 simulated data sets and estimates of the parameters were compared with the values used in MMID4 to generate the residue curves.

RESULTS

Data Simulation

The simulated data exhibit many of the characteristics of the experimental data (Fig. 1). Indeed the simulated data match the example data very well despite the arterial input function used (a single simulated input not determined in individual subjects). The physiological parameters influence the residue curves in different ways (Fig. 2). The initial slope of the residue curve is determined principally by the vascular parameters. The early curvature and peak observed in the data is strongly influenced by PS. There is, however, considerable overlap of these effects.

Model Fitting

Models 1 and 2 fitted the simulated data in a reproducible manner. Parameter estimates obtained from these fits are displayed in Fig. 3. Parameter estimates obtained using model 3 were not always unique, and often depended on the starting guesses used in the fitting routine. This implies a significant correlation between parameters and the existence of local minima (22). To improve the stability of the regression procedure, an approach similar to that de-

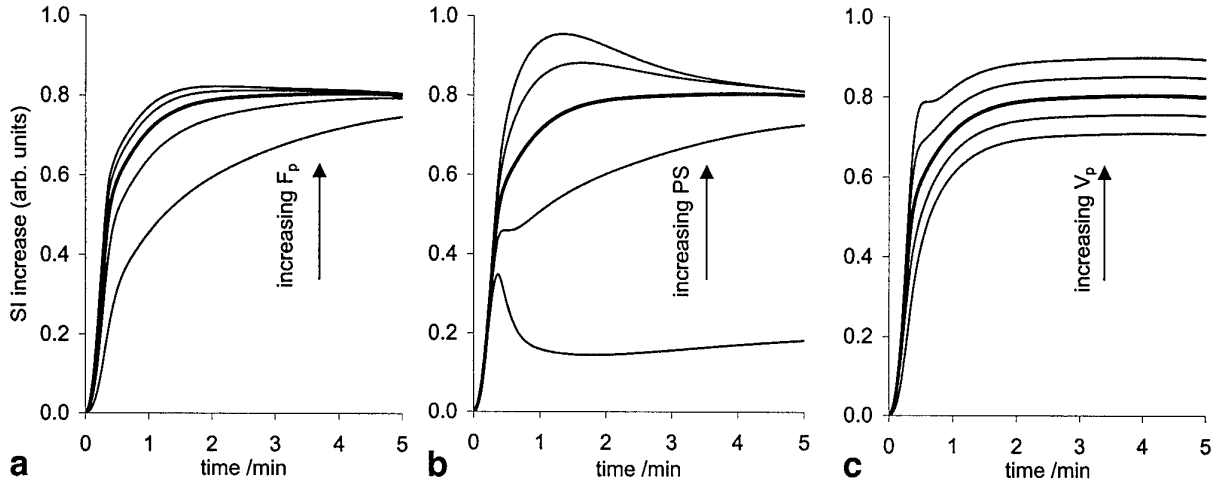

FIG. 2. Influence of the physiological parameters. The shape of the signal-time curve is modified by changes in the values of individual parameters. The baseline curve (bold line) is representative of data acquired from a breast tumor. The influence of changes in (**a**) plasma flow (F_p), (**b**) permeability-surface area product (PS), and (**c**) plasma volume (V_p) are shown. The parameter values used to generate the curves are detailed in Table 1a.

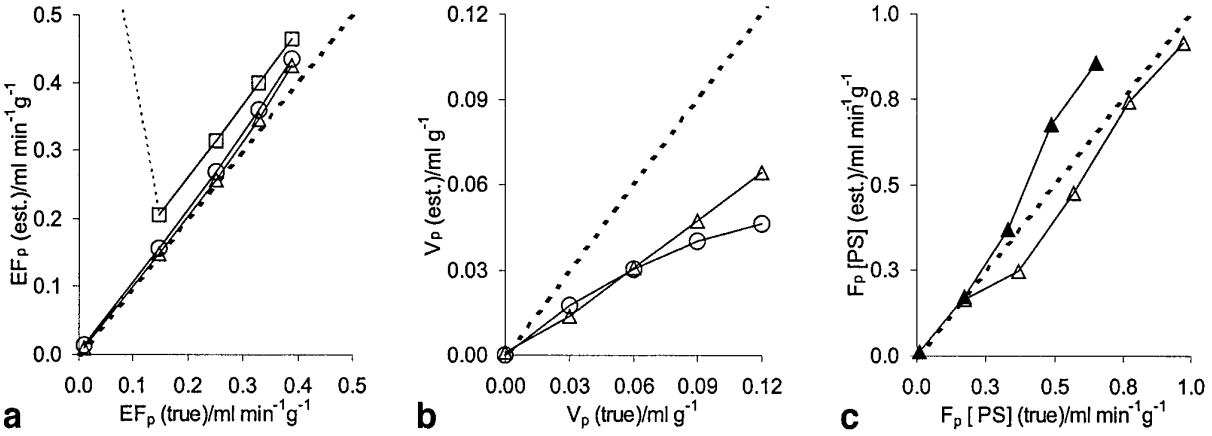

FIG. 3. Parameter estimates as a function of the "true" values. Estimates of the parameters (**a**) EF_p, (**b**) V_p, and (**c**) F_p and PS obtained by fitting model 1 (squares), model 2 (circles), and model 3 (triangles) to the simulated data (Table 1a). The open triangles in **c** represent estimates of F_p, the filled triangles represent estimates of PS, and the dashed lines in all figures represent lines of identity. Similar plots were obtained using the parameters of Table 1b. **a:** Note the failure of model 1 at low EF_p (0.01 ml $min^{-1}g^{-1}$). The model 1 estimate is off-scale at 0.82 ml $min^{-1}g^{-1}$.

scribed by Henderson et al. (22) was adopted. Multiple fits were performed using a range of starting points (i.e., different initial estimates of τ). The final solution selected was that which minimized the sum of squared differences between the data and the model fit. Representative results are displayed in Fig. 3. Though the results in general were convoluted, certain trends were apparent. In particular, V_p was consistently underestimated by both model 2 and model 3 (by between 2% and 96%). The parameters of model 3 became less accurate at low flow or high permeability, where PS tended to be overestimated (to an extreme of 152%) and F_p was slightly underestimated (up to 34%).

DISCUSSION

Increasing numbers of investigators are employing models to analyze their dynamic contrast-enhanced data (20). It is important that the techniques used are fully understood so that they may benefit other investigators. Part of this process is to investigate the physiological interpretation of these parameters. Typically, this would be achieved by comparison of the MRI results with a "gold standard." However, suitable techniques for comparison are difficult to find. PET has often been quoted as a gold standard technique for measurement of blood flow (8), but the techniques used to interpret PET data are very similar to those now used in MRI and can suffer from similar pitfalls (5). In this study, a realistic, established model has been used to simulate tissue residue curves that closely match existing experimental data. In this way, data were generated with known physiological variables that were independent of the models subsequently used to interpret them.

Data Simulation

MMID4 is clearly capable of generating residue curves that closely match experimental data acquired by MRI (8,14,23) (Fig. 1). This should not be interpreted as suggesting that MMID4 fully describes the physiology of the tumors studied. It is simply a step towards that goal. However, MMID4 does incorporate parameters of particular interest: F_p, PS, V_e, and V_p, and each influences the residue curve over differing temporal ranges and in subtly different ways (Fig. 2). F_p, for example, determines the initial slope of the residue curves simulated in this study. PS has a more convoluted impact depending upon the ratio PS:F_p. Certainly, the curvature of the residue curve about the initial peak (Fig. 2) is strongly influenced by PS. V_e has perhaps the clearest affect upon the residue curve. Increasing V_e tends to delay the rise of the curve to its equilibrium amplitude. Finally, the impact of V_p is seen throughout the time course. It is the overlap in influence of each variable that complicates the issue of parameter estimation.

Model Fitting

A model, by definition, is a practical simplification of the true tissue physiology; as a result it is, to some extent, flawed. It is therefore not surprising that the simple models tested were unable to provide accurate estimates of the physiological parameters in all cases. Model 3 bears the closest resemblance to MMID4 but clearly fails to describe the more complex model in certain circumstances. In particular, model 3 systematically underestimates V_p and overestimates PS under conditions of low flow or high permeability (Fig. 3). This may be a consequence of flow heterogeneity (14), an effect all three models overlook. Flow heterogeneity differs between regions and individuals and may not remain constant, as assumed in this study, but could change as a function of pathology (8). The effect of additional disrupting influences on the input function—delay and dispersion—have, for the sake of conciseness, not been considered in this study since their influence upon parameter estimation has been studied elsewhere (7).

If the direct vascular contribution to the signal is ignored (model 1), EF_p (also known as K^{trans} (20)) is overestimated (by up to 54% (Fig. 3a)). Indeed, under certain circum-

stances model 1 breaks down completely. However, to measure the vascular signal contribution it is essential to measure the vascular input and acquire data with a high temporal resolution (6). The choice of model 3 for data analysis requires a sampling interval less than the mean transit time of the tracer. Once the sampling interval reaches the mean transit time, model 3 may be simplified to a form similar to model 2 (21). It is clear from Fig. 3 that the use of model 2, despite the inclusion of a vascular contribution, leads to consistent underestimation of V_p and a slight overestimation of EF_p. These findings mirror the results of a previous study (21). Interestingly, the ratio EF_p:V_e may be estimated with an error of less than 10%, which is consistently less than the error in the estimate of EF_p alone (data not shown). This ratio, otherwise referred to as k_{ep} (20), may be estimated without a tissue T_1 measurement (19), and has been identified as a useful parameter for differential diagnosis in the study of primary breast tumors (24).

Another important issue, which is not always apparent to the investigator, is the uniqueness of the model solution (23). Many of the estimates obtained, using model 3, varied as a function of the starting values used for curve fitting. The array of local minima result from parameter correlations, i.e., different combinations of the parameters produce very similar solutions. Parameter correlations may be examined using sensitivity functions (13) or by examination of the fit correlation matrix. Parameter estimation is simplified if the complexity of the fit can be reduced. It is possible to use MMID4 for data analysis (14,23), but the issue of parameter uniqueness is further complicated by the surfeit of possible parameter combinations. Jerosch-Herold et al. (23), studying myocardial blood flow and capillary permeability in a porcine model, found that they were unable to obtain unique estimates of blood flow, volume, and PS using an extracellular contrast agent (Gd-DTPA). They were able to assess blood flow using an experimental intravascular tracer, as all the extravascular parameters were eliminated as degrees of freedom of the model. Even under these circumstances, it was necessary to fix the value of numerous additional MMID4 parameters at literature values (23). It is likely that future studies may benefit from the combined use of intravascular and extracellular tracers in multiple-indicator-type modeling (13). Indeed, model 3 has been tested with two different contrast agents (22) in a canine model of breast cancer. Furthermore, Henderson et al. (22) recognized the confounding impact of parameter correlations upon parameter estimation. To overcome this problem, curve fitting was performed in a serial fashion using a succession of starting points for the fit (22), a policy adopted in this study.

Implications for Tracer Kinetic Studies

It is important at the outset of a study to identify the most relevant parameters to measure. Without an arterial input function and with limited temporal resolution, the Tofts and Kermode (9) and Larsson et al. (19) models have proved very useful. In tissues with a negligible blood volume they may also provide good estimates of EF_p. However, with a measured arterial input function and rapid data collection, model 2 may be a more appropriate model

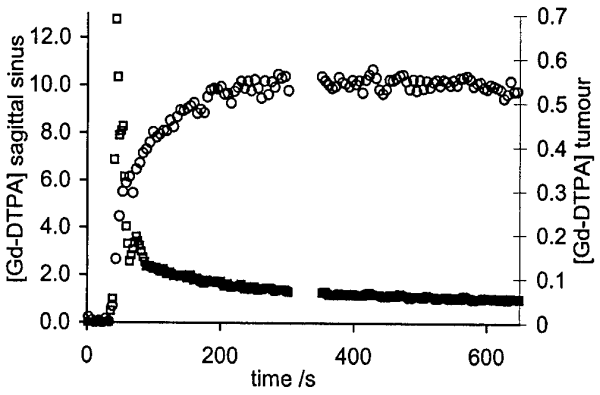

FIG. 4. Measurement of the arterial and tissue concentrations in vivo. Given an appropriate imaging sequence the arterial input function and the tissue residue curve can be measured in vivo. These data were acquired from regions of interest encompassing the sagittal sinus (open squares) and a meningioma (open circles). Calculation of the concentration of Gd-DTPA (mM) was based upon precontrast T_1 measurement (12).

for clinical data evaluation. In either case the investigator must appreciate the assumptions and implications of using these models. In particular, neither model provides separate estimates of perfusion and permeability. These parameters are inextricably combined in the EF_p product. The model (model 3) of St. Lawrence and Lee (21) offers the possibility of assessing blood flow and extraction simultaneously, but may require carefully constrained supervised data fitting (22), additional measurements, or multiple tracers to overcome problems with parameter correlations (23). In all cases it is essential to collect appropriate data of the highest quality if accuracy and precision are to be attained.

As a practical example of these choices, the models were each fitted to recent experimental data (input and tissue residue curves) acquired in a meningioma (12), shown in Fig. 4. These data were simultaneously acquired every 5.1 s in the sagittal sinus and tumor using a T_1-weighted 3D gradient-echo sequence (TR = 4.3 ms, TE = 1.1 ms, flip angle = 35°) on a 1.5 T MR system. The signal from the sagittal sinus was used as input to the models (a vein was chosen for simplicity and is merely illustrative) and the effective sampling interval was halved by linear interpolation. The following parameter estimates were obtained using model 3: blood (rather than plasma) flow, F_b = 0.25 ml $min^{-1}g^{-1}$; blood volume, V_b = 0.02 ml g^{-1}; V_e = 0.43 ml g^{-1}; and PS = 0.14 ml $min^{-1}g^{-1}$. It is unclear whether the interpolation step was required since the capillary transit time, τ, was estimated to be 4.8 s. Based on the results of the previous simulation exercise, PS and F_b may be somewhat overestimated and underestimated, respectively. Furthermore, the estimate of V_b is likely to represent a significant underestimate. However, the product EF_b (= 0.16 ml $min^{-1}g^{-1}$) is likely to be accurately estimated, and these results compare well with estimates obtained using model 2: EF_b = 0.16 ml $min^{-1}g^{-1}$; V_b = 0.02 ml g^{-1}; and V_e = 0.44 ml g^{-1}. Predictably, the estimate of the EF_b product made by model 1 was larger (0.18 ml

$min^{-1}g^{-1}$) but a comparable value was obtained for V_e (0.44 ml g^{-1}). Unless an independent estimate of blood flow or permeability is essential, model 2 may be an appropriate choice for analysis of these data since it requires neither data interpolation nor supervised fitting.

CONCLUSIONS

The use of models for tracer kinetic analysis potentially enables the investigator to interpret MR data in physiological terms. However, both the measurement process and the data analysis introduce a degree of uncertainty into parameter estimation. Simplified models, some of which are in common use, may not provide accurate estimates of the physiological parameters of interest. It is important to address these uncertainties because it is only after the parameters of the model have been accurately estimated that the diagnostic or prognostic efficacy of specific quantitative physiological parameters can be properly tested.

ACKNOWLEDGMENTS

Preliminary studies were carried out in the laboratory of Steve Blackband, Department of Neuroscience, University of Florida. I am grateful to Xiao Ping Zhu, Ka-Loh Li, and Alan Jackson, University of Manchester, for kindly providing example data, and to Keith St. Lawrence, Geoff Parker, and Stephen R. Williams for their insightful comments. The National Simulation Resource is supported by the NIH (RR-01243).

REFERENCES

1. Parker GJM, Tofts PS. Pharmacokinetic analysis of neoplasms using contrast-enhanced dynamic magnetic resonance imaging. Top Magn Reson Imaging 1999;10:130–143.
2. Fritz-Hansen T, Rostrup E, Sondergaard L, Ring PB, Amtorp O, Larsson HBW. Capillary transfer constant of Gd-DTPA in the myocardium at rest and during vasodilation assessed by MRI. Magn Reson Med 1998; 40:922–929.
3. Buckley DL, Drew PJ, Mussurakis S, Monson JRT, Horsman A. Microvessel density in invasive breast cancer assessed by dynamic Gd-DTPA enhanced MRI. J Magn Reson Imaging 1997;7:461–464.
4. van der Sanden BPJ, Rozijn TH, Rijken PFJW, Peters HPW, Heerschap A, van der Kogel AJ, Bovee WMMJ. Noninvasive assessment of the functional neovasculature in 9L-glioma growing in rat brain by dynamic H-1 magnetic resonance imaging of gadolinium uptake. J Cereb Blood Flow Metab 2000;20:861–870.
5. Larson KB, Markham J, Raichle ME. Tracer-kinetic models for measuring cerebral blood flow using externally detected radiotracers. J Cereb Blood Flow Metab 1987;7:443–463.
6. Henderson E, Rutt BK, Lee TY. Temporal sampling requirements for the tracer kinetics modeling of breast disease. Magn Reson Imaging 1998; 16:1057–1073.
7. Calamante F, Gadian DG, Connelly A. Delay and dispersion effects in dynamic susceptibility contrast MRI: simulations using singular value decomposition. Magn Reson Med 2000;44:464–473.
8. Ostergaard L, Chesler DA, Weisskoff RM, Sorensen AG, Rosen BR. Modeling cerebral blood flow and flow heterogeneity from magnetic resonance residue data. J Cereb Blood Flow Metab 1999;19:690–699.
9. Tofts PS, Kermode AG. Measurement of the blood-brain barrier permeability and leakage space using dynamic MR imaging. I. Fundamental concepts. Magn Reson Med 1991;17:357–367.
10. Parker GJM, Tanner SF, Leach MO. Pitfalls in the measurement of tissue permeability over short time-scales using a low temporal resolution blood input function. In: Proceedings of the 4th Annual Meeting of ISMRM. New York, 1996. p 1582.
11. Fritz-Hansen T, Rostrup E, Larsson HB, Sondergaard L, Ring P, Henriksen O. Measurement of the arterial concentration of Gd-DTPA using MRI: a step toward quantitative perfusion imaging. Magn Reson Med 1996;36:225–231.
12. Li K-L, Zhu XP, Waterton J, Jackson A. Improved 3D quantitative mapping of blood volume and endothelial permeability in brain tumors. J Magn Reson Imaging 2000;12:347–357.
13. Bassingthwaighte JB, Goresky CA. Modeling in the analysis of solute and water exchange in the microvasculature. In: Renkin EM, Michel CC, Geiger SR, editors. Handbook of physiology. Section 2. The cardiovascular system. Bethesda: American Physiological Society; 1984. p 549–626.
14. Kroll K, Wilke N, Jerosch-Herold M, Wang Y, Zhang Y, Bache RJ, Bassingthwaighte JB. Modeling regional myocardial flows from residue functions of an intravascular indicator. Am J Physiol 1996;271:H1643–H1655.
15. Buckley DL. Modelling contrast uptake by neoplasms using dynamic magnetic resonance imaging. Ph.D. thesis, University of Hull; 1996.
16. Jain RK. Determinants of tumor blood flow: a review. Cancer Res 1988;48:2641–2658.
17. Tofts PS. Modeling tracer kinetics in dynamic Gd-DTPA MR imaging. J Magn Reson Imaging 1997;7:91–101.
18. Kety SS. The theory and applications of the exchange of inert gas at the lungs and tissues. Pharmacol Rev 1951;3:1–41.
19. Larsson HBW, Stubgaard M, Frederiksen JL, Jensen M, Henriksen O, Paulson OB. Quantitation of blood-brain barrier defect by magnetic resonance imaging and gadolinium-DTPA in patients with multiple sclerosis and brain tumors. Magn Reson Med 1990;16:117–131.
20. Tofts PS, Brix G, Buckley DL, Evelhoch JL, Henderson E, Knopp MV, Larsson HB, Lee TY, Mayr NA, Parker GJ, Port RE, Taylor J, Weisskoff RM. Estimating kinetic parameters from dynamic contrast-enhanced T_1-weighted MRI of a diffusable tracer: standardized quantities and symbols. J Magn Reson Imaging 1999;10:223–232.
21. St. Lawrence KS, Lee TY. An adiabatic approximation to the tissue homogeneity model for water exchange in the brain. I. Theoretical derivation. J Cereb Blood Flow Metab 1998;18:1365–1377.
22. Henderson E, Sykes J, Drost D, Weinmann HJ, Rutt BK, Lee TY. Simultaneous MRI measurement of blood flow, blood volume, and capillary permeability in mammary tumors using two different contrast agents. J Magn Reson Imaging 2000;12:991–1003.
23. Jerosch-Herold M, Wilke N, Wang Y, Gong GR, Mansoor AM, Huang H, Gurchumelidze S, Stillman AE. Direct comparison of an intravascular and an extracellular contrast agent for quantification of myocardial perfusion. Int J Card Imaging 1999;15:453–464.
24. Mussurakis S, Buckley DL, Drew PJ, Fox JN, Carleton PJ, Turnbull LW, Horsman A. Dynamic MR imaging of the breast combined with analysis of contrast agent kinetics in the differentiation of primary breast tumours. Clin Radiol 1997;52:516–526.

The influence of transcapillary water exchange on the analysis of tracer kinetics in dynamic Gd-DTPA-enhanced T_1-weighted MRI

David L. Buckley
Imaging Science and Biomedical Engineering, University of Manchester, Manchester, U.K.

Abstract

Though it is known that water exchange plays a major role in determining the MR signal obtained in contrast agent studies there is no consensus on the significance of it's effects in typical studies. Using data measured in gliomas a simulation was performed to assess the influence of slow transcapillary water exchange on the modeling of Gd-DTPA enhanced T1 data. Even when using an exchange-minimization imaging sequence, parameter estimates were disrupted by exchange. However, under conditions of significant Gd-DTPA extraction the extraction-flow product remained relatively accurate.

Introduction

Water exchange plays a major role in determining the signal changes measured in contrast-enhanced MRI [1,2]. It is generally acknowledged that transcytolemmal exchange remains fast under most circumstances [1], though this remains somewhat controversial. However, most investigators recognize that transcapillary exchange can have a significant influence upon the MR signals they measure [2,3] yet often assume that the effects of intermediate to slow exchange will not be significant in their research. A simulation study was undertaken to examine the influence of slow transcapillary exchange on estimates of the tracer kinetic parameters that may be obtained from dynamic Gd-DTPA enhanced imaging of the brain [4].

Methods

Concentration-time data representing the interstitial and vascular spaces of four different tissue types were simulated using an input function previously measured in the brain [4] and a distributed pathway model of tracer kinetics (MMID4, made available by the National Simulation Resource [5]). Each tissue type {glioma1 (high extraction), glioma2 (low extraction), normal gray and normal white matter} had associated with it representative values of blood flow (F), blood volume (V_b), vessel permeability-surface area product (PS) and interstitial volume (V_e) (Fig. 1).

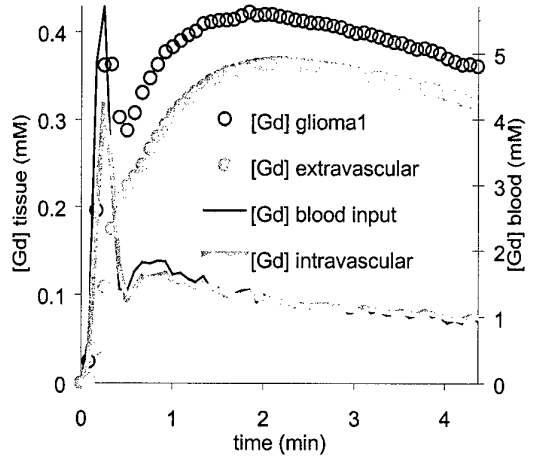

Figure 1. Input and tissue compartment concentration-time curves for glioma1. The curves were simulated using physiological parameters: F, 0.43 ml/g/min; V_b, 0.06 ml/g; PS, 0.13 ml/g/min; V_e, 0.15 ml/g (extraction fraction, E = 0.42).

These data were subsequently used to generate whole tissue signal-time curves using an equation describing a FLASH sequence (TR, 4.3 ms; flip angle, 35° [4]) and assuming either fast or slow water exchange (i.e., mono- or biexponential T1 recovery, respectively). Finally, each whole tissue signal-time curve was converted back to a concentration-time curve under the conventional assumption of fast water exchange [3]. A tracer kinetic model [6] was then fitted to these processed data to arrive at exchange-mediated estimates of F, V_b, PS and V_e.

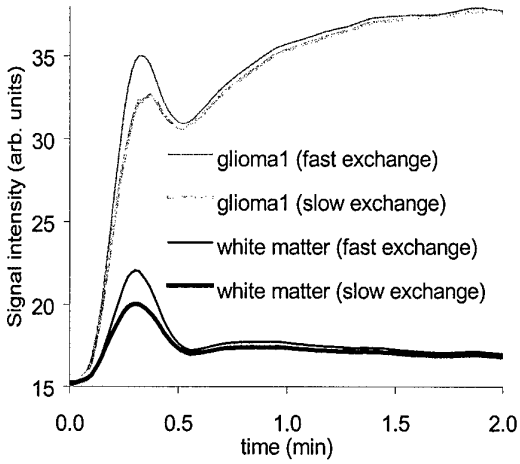

Figure 2. Simulated signal-time curves for glioma1 (Fig. 1) and normal white matter resulting from a FLASH acquisition (TR, 4.3 ms, flip 35°) and either fast or slow transcapillary water exchange.

Results & Discussion

As previously reported [2,3], the effect of slow exchange was to flatten the first pass response of the signal-time curves (Fig. 2). This resulted in systematic underestimation of F and V_b and overestimates of PS (and thus E). Overestimates of the EF product (K^{trans}) and V_e were slight [3]. Disturbingly, the non-linear effect of slow exchange on the normal gray and white matter signal-time curves was to erroneously imply mild blood-brain barrier breakdown (E > 0).

These findings support previous studies and highlight the importance of exchange in contrast enhanced T1 imaging. Furthermore, it is important to note that the errors associated with slow exchange compound those already associated with the use of kinetic modeling [7] and suggest that estimates of blood volume using such approaches are appreciably error prone.

Acknowledgments

Supported by the U.S. DoD Prostate Cancer Research Program (PC991154). The National Simulation Resource is supported by the NIH (RR-01243). Thanks to Hamied Haroon & Alan Jackson.

References

1. Donahue et al., *Magn Reson Med* **32**:66 (1994)
2. Judd et al., *Magn Reson Med* **41**:334 (1999)
3. Larsson et al., *Magn Reson Med* **46**:272 (2001)
4. Li et al., *J Magn Reson Imaging* **12**:347 (2000)
5. Kroll et al., *Am J Physiol* **271**:H1643 (1996)
6. St. Lawrence & Lee, *J Cereb Blood Flow Metab* **18**:1365 (1998)
7. Buckley, *Magn Reson Med* In Press (2002)